Research Article

The Journal of Comparative Neurology
Research in Systems Neuroscience
DOI 10.1002/cne.23129

Selective distribution of $GABA_A$ receptor subtypes in mouse spinal dorsal horn neurons and primary afferents

Jolly Paul[1], Hanns Ulrich Zeilhofer[1,2], Jean-Marc Fritschy[1*]

[1]Institute of Pharmacology and Toxicology, University of Zurich, Winterthurerstrasse 190, CH-8057 Zurich, Switzerland, and Neuroscience Center Zurich

[2]Institute of Pharmaceutical Sciences, Swiss Federal Institute of Technology ETH Zurich, Wolfgang-Pauli-Strasse 10, CH-8093 Zurich, Switzerland

Running head: $GABA_A$ receptors in the spinal cord dorsal horn

Associate Editor: Gert Holstege

*Corresponding author:

Tel. 0041 44 635 5926; Fax. 0041 44 635 6874; e-mail: fritschy@pharma.uzh.ch

Keywords: GABAergic synapse; presynaptic receptor; gephyrin; CGRP; IB4; pain; nociception

Support: This study was supported by grants from the Swiss National Science Foundation (31003AB_131093 to HUZ and 31003A_130495 to JMF).

Received: Dec 12, 2011; Revised: Apr 12, 2012; Accepted: Apr 13, 2012

Abstract

In the spinal cord dorsal horn, presynaptic $GABA_A$ receptors ($GABA_AR$) in the terminals of nociceptors as well as postsynaptic receptors in spinal neurons regulate the transmission of nociceptive and somatosensory signals from the periphery. $GABA_AR$ are heterogeneous and distinguished functionally and pharmacologically by the type of α subunit variant they contain. This heterogeneity raises the possibility that $GABA_AR$ subtypes differentially regulate specific pain modalities. Here, we characterized the subcellular distribution of $GABA_AR$ subtypes in nociceptive circuits using immunohistochemistry with subunit-specific antibodies combined with markers of primary afferents and dorsal horn neurons. Confocal laser scanning microscopy analysis revealed a distinct, partially overlapping laminar distribution of the α1-3 and α5 subunit-immunoreactivity in laminae I-V. Likewise, a layer-specific pattern was evident for their distribution among glutamatergic, GABAergic, and glycinergic neurons (detected in transgenic mice expressing vGluT2-eGFP, GAD67-eGFP, and GlyT2-eGFP, respectively). Finally, all four subunits could be detected within primary afferent terminals. C-fibers predominantly contained either α2 or α3 subunit-immunoreactivity, terminals from myelinated (Aβ/Aδ) fibers were co-labeled in roughly equal proportion with each subunit. Presence of axo-axonic GABAergic synapses was determined by co-staining with gephyrin and vesicular inhibitory amino acid transporter to label GABAergic postsynaptic densities and terminals, respectively. Co-localization of α2 or α3 subunit with these markers was observed in a subset of C-fiber synapses. Furthermore, gephyrin mRNA and protein expression was detected in dorsal root ganglia. Collectively, these results show that differential $GABA_AR$ distribution in primary afferent terminals and dorsal horn neurons allows for multiple, circuit-specific modes of regulation of nociceptive circuits.

Introduction

Chronic pain is a frequent, strongly debilitating condition that is often resistant to pharmacotherapy and therefore a major socio-economic problem. Chronic pain can result from inflammation, nerve injury, or CNS lesion. Noxious stimuli evoking pain are detected by two major classes of nociceptors, Aδ and C nociceptors, whose cell bodies are located in dorsal root ganglia (DRG) and trigeminal ganglia. The central axons of DRG-residing nociceptors terminate mainly in the superficial layers of the spinal dorsal horn (laminae I and II) (Rexed, 1952), with peptidergic and non-peptidergic C fibers being segregated in lamina II outer (IIo) and II inner (IIi), respectively (Hunt and Mantyh, 2001; Todd, 2010). The spinal cord dorsal horn processes nociceptive signals and relays them to higher brain centers, where conscious pain sensation arises. Chronic pain is a pathological condition involving altered function of primary nociceptors and of central pain circuits, manifesting in primary hyperalgesia (exaggerated pain sensations at the site of injury) and secondary hyperalgesia in uninjured healthy tissue.

In 1965, Melzack and Wall proposed the gate control theory of pain attributing a critical contribution of inhibitory interneurons (GABAergic and glycinergic) of the spinal dorsal horn in regulating nociceptive signal strength and keeping nociceptive and non-nociceptive modalities apart (Melzack and Wall, 1965). Intrathecally-applied bicuculline and strychnine, blockers of $GABA_A$ receptors ($GABA_AR$) and glycine receptors respectively, increase nociceptive reactions elicited by exposure to noxious stimuli (Roberts et al., 1986; Yaksh, 1989). Conversely, enhancing $GABA_AR$ function by spinal application of GABA or a positive allosteric modulator, such as midazolam, was shown to depress noxious stimulus-evoked activity in spinal cord neurons and to reverse neuropathic pain induced by nerve injury (Clavier et al., 1992; Eaton et al., 1999; Knabl et al., 2008; Sumida et al., 1995).

$GABA_ARs$ are ligand-gated heteropentameric ion channels assembled from a repertoire of 19 subunits (α1-6, β1-3, γ1-3, δ, ε, θ, π, ρ1-3). The most common subtype in the CNS is composed of two α, two β, and one γ subunit (Möhler, 2006). $GABA_AR$ containing α1, α2, α3, or α5 subunits associated with the γ2 subunit are sensitive to diazepam (Wieland et al., 1992). In the spinal cord, morphological studies revealed a considerable heterogeneity in the distribution of $GABA_AR$ subunits. Thus,

in the rat, *in situ* hybridization studies detected strong signals for $GABA_AR$ α2, α3, β3 and γ2 subunit mRNA, weak expression for α1, α5, β1, β2, γ1 and γ3, and could not detect α6 and δ subunits (Ma et al., 1993; Persohn et al., 1991; Wisden et al., 1991). Immunohistochemical analysis revealed distinct laminar distribution of major α subunit variants (Bohlhalter et al., 1996).

$GABA_AR$ can modulate spinal nociceptive processing via at least two mechanisms. Postsynaptic $GABA_AR$ in spinal cord neurons directly reduce their excitability, while $GABA_AR$ located in afferent terminals of nociceptors cause presynaptic inhibition of transmitter release. Previous work has demonstrated that the α2 and α3 subunits are abundant in mouse dorsal horn neurons (Knabl et al., 2008), co-localized in part with substance P-positive terminals in lamina II and with NK1-receptor-positive lamina I neurons. In addition, there is extensive pharmacological and behavioral evidence indicating that both modes of inhibition contribute to physiological and pathological pain sensation (Jasmin et al., 2003; Knabl et al., 2008; Munro et al., 2011; Sastry, 1980; Zeilhofer et al., 2012b). However, the precise site of action of the different $GABA_AR$ subtypes in various pain modalities is not known.

These uncertainties are due, in large part, to insufficient knowledge about the cellular and subcellular distribution of $GABA_AR$ subtypes in circuits of spinal dorsal horn (Zeilhofer et al., 2012b). Therefore, the aim of this study was to analyze immunohistochemically the molecular organization of $GABA_AR$ in identified intrinsic dorsal horn neurons and primary afferents in layers I-III, using immunofluorescence staining combined with specific neuronal and axonal markers.

Materials and Methods

Animals

Experiments were performed with 6-8 week old C57BL/6J male and female mice. For identification of glutamatergic, GABAergic and glycinergic neurons, transgenic mice expressing vGlut2-eGFP (www.gensat.org, (Gong et al., 2003), GAD67-eGFP (Tamamaki et al., 2003; Wang et al., 2009) and GlyT2-eGFP (Zeilhofer et al., 2005) on C57BL/6J background were used. Mice were bred in the animal facility of Institute of Pharmacology and Toxicology under the approval of local authorities. They were maintained under standard conditions with 12 h day/night cycle and *ad libitum* supply of food and water. All experimental procedures were approved by the Cantonal Veterinary Office of Zurich.

Western blot analysis

Mice (n=3) deeply anaesthetized by intraperitoneal administration of sodium pentobarbital (50 mg/kg) were decapitated and DRG were quickly dissected out, snap-frozen with dry ice, and stored at -80°C until further processing. 30-40 DRG were homogenized in ice-cold solubilization buffer (1 mM EDTA, 10 mM Tris Cl, 150 mM NaCl, 0.02% NaN_3) followed by sonication. The protein content of the sonicated sample was determined by Bradford's assay and was then denatured using 10% mercaptoethanol. The samples were then serially diluted to achieve the required protein concentration in 20 µL loading volume. 7.5% SDS-polyacrylamide gels were used for electrophoresis and a wet-blot was developed on nitrocellulose acetate membrane. The membrane was then blocked using 5% western blocking reagent (Roche Diagnostics GmbH, Mannheim, Germany, Cat No. 11 921 673 001) in Tris buffered saline-Tween 20 followed by overnight incubation in mouse monoclonal antibody 7a against gephyrin (Table 1). Following washing, the membrane was treated with secondary antibody goat anti-mouse conjugated to horseradish peroxidase (1:300 dilution) and the signal was enhanced using freshly prepared chemiluminescent mix (Super signal West Pico chemiluminescent substrate, Thermo, 3747N, Rockford, Cat No. 34087). The images were captured using Fujifilm scanner using the software Fujifilm-image reader LAS 100 Pro V2.51. Mouse crude brain homogenates were included in the test as positive control for gephyrin detection and albumin as a negative control.

Real-time PCR

Lumbar DRG from adult mice were removed following decapitation and collected in a tube containing a lysis solution. Total RNA was isolated by using GenElute™ Mammalian Total RNA Miniprep Kit (RTN70, Sigma-Aldrich). Genomic DNA was removed and cDNA was generated in a reaction mixture using QuantiTect® Reverse Transcription Kit (Qiagen® GmbH, Hilden, Germany, Cat. No. 205311), real-time quantitative PCR (qPCR) was performed and analyzed using TaqMan® gene expression master mix (Applied Biosystems International, Inc., Rotkreuz, Switzerland, Part No. 4369016) with generated cDNA in a total reaction volume of 10 µL in 384-well arrays with 7900HT fast real-time PCR system and software (Applied Biosystems). mRNA expression of gephyrin was quantified using pre-designed coding assays (FAM™ dye-labeled TaqMan® MGB probes; Applied Biosystems) (glyceraldehyde-3-phosphate dehydrogenase (GAPDH), cytoplasmic reference gene: assay ID: Mm99999915_g1, context sequence: GAACGGATTTGGCCGTATTGGGCGC; gephyrin: assay ID: Mm01297308_m1**, context sequence: AGAAAGGATC TCAGGAATGCTTTCA). The real-time qPCR cycling program consisted of 95°C for 10 min, followed by 40 cycles of 95°C for 15 s and 60°C for 1 min. The expression level of gephyrin gene was normalized to that of the GAPDH gene, which was used as a reference. All qPCR reactions were carried out in triplicate. Relative quantification of transcript was determined using the comparative CT method ($2^{-\Delta CT}$) calibrated to β-actin.

Immunohistochemistry

Immunohistochemistry was performed using well characterized primary antibodies described in table 1. The distribution of α subunit variants in the lumbar spinal cord was analyzed in sections processed for immunoperoxidase staining. Mice were deeply anaesthetized with pentobarbital (nembutal, 50 mg/kg, i.p.) followed by transcardiac perfusion of saline (20 mL) and 70 mL ice-cold fixative containing 4% paraformaldehyde (PFA) and 15% saturated picric acid solution in 0.15 M sodium phosphate buffer, pH 7.4. The spinal cords were extracted immediately after the perfusion and post-fixed in the same solution for 5 h. Tissue was then processed for antigen retrieval as described (Kralic et al., 2006), cryo-protected with 30% sucrose in phosphate-buffered saline (PBS), and cut coronally at 40 µm from frozen blocks with a sliding microtome. Sections were collected in PBS and stored at -20°C in antifreeze

solution (15% glucose and 30% ethylene glycol in 50 mM sodium phosphate buffer, pH 7.4) prior to use. Sections were incubated free-floating overnight at 4°C with primary antibodies against $GABA_AR$ subunits (Table 1) in Tris buffer pH 7.7 containing 2% normal goat serum and 0.2% Triton X-100. Sections were then washed and incubated for 30 min at room temperature with biotinylated secondary antibodies (1:300; Jackson ImmunoResearch, West Grove, PA), followed by incubation in avidin-biotin complex (1:100 in Tris buffer, Vectastain Elite Kit; Vector Laboratories, Burlingame, CA), for 30 min, washed again and finally visualized with diaminobenzidine tetrahydrochloride (DAB; Sigma, St Louis, MO) in Tris buffer (pH 7.7) containing 0.015% hydrogen peroxide. The color reaction was stopped after 5–15 min with ice-cold PBS. Sections were then mounted on gelatin-coated slides and air-dried followed by dehydration with ethanol. The slides were then cleared in xylol and cover-slipped with Eukitt (Erne Chemie, Dallikon, Switzerland).

The distribution of $GABA_AR$ α subunits in identified spinal cord neurons were analyzed by immunofluorescence staining on coronal sections of transgenic eGFP-expressing mice. The sections were prepared from 2-3 male mice as described above. For staining, the sections were incubated overnight at 4°C with a mixture of primary antibodies diluted in Tris buffer containing 2% normal goat serum. Sections were washed extensively and incubated for 1h at room temperature with the corresponding secondary antibodies conjugated to Cy3 (1:500), Cy2 (1:200) (Jackson ImmunoResearch) and or Alexa488 (1:1000, Molecular Probes, Eugene, OR). Sections were washed again and cover-slipped with fluorescence mounting medium (DAKO, Carpinteria, CA).

Distribution of $GABA_AR$ α subunits within primary afferent terminals was studied using a protocol developed for detection of postsynaptic proteins (Schneider Gasser et al., 2006). Mice were deeply anaesthetized with pentobarbital (nembutal, 50 mg/kg, i.p.) and perfused with Ringer's solution. Spinal cords were rapidly collected by pressure ejection and placed in oxygenated ice-cold artificial cerebrospinal fluid. 300 µm thick parasagittal slices were prepared from the lumbar spinal cord with a vibrating microtome and incubated for 45 min at 34°C. They were then fixed in 4% paraformaldehyde in 0.1 M sodium phosphate buffer for 10 min, extensively washed, and stored overnight in 30% sucrose in Tris buffer for cryo-protection. Slices were then flat-frozen and sections were cut at 14 µm with a cryostat, mounted on gelatin-

coated glass slides and air-dried at room temperature for 45 min. Immunofluorescence staining was performed as described above.

Image acquisition and analysis

The regional distribution of α subunit-immunoreactivity (-IR) analyzed by immunoperoxidase staining was visualized in sections from four mice with bright field microscopy (Axioplan; Zeiss) using MCID Elite 6.0 software (Imaging Research, GE Healthcare Bio-Sciences AB, Uppsala, Sweden) for image acquisition. Images were cropped to the desired dimensions in Adobe Photoshop CS. Minimal adjustments of contrast and brightness were applied to entire images, if needed.

Double and triple-immunofluorescence signals were visualized by confocal microscopy (LSM 710; Zeiss AG, Jena, Germany) using a 63× Plan-Apochromat objective (N.A. 1.4). The pinhole was set to 1 Airy unit for each channel and separate color channels were acquired sequentially. The acquisition settings were adjusted to cover the entire dynamic range of the photomultipliers. Typically, stacks of confocal images (1024×1024 pixels) spaced by 0.3 µm were acquired at a magnification of 56-130 µm/pixel. For display, images were processed with the image analysis software Imaris (Bitplane; Zurich, Switzerland). Images from all channels were overlaid (maximal intensity projection) and background was subtracted, when necessary. A low-pass filter was used for images displaying α subunit staining.

Analysis of the distribution of α subunit-IR in eGFP-positive neurons and dendrites was performed in single confocal sections from 2-3 mice per genotype acquired at a magnification of 78 nm/pixel in 8-bit gray scale images, using a threshold segmentation algorithm (minimal intensity, 90–130; area >0.08 μm^2). All structures with >70% overlap between both channels (co-localized area >0.056 μm^2, corresponding to 9 pixels) was apparent were considered as "colocalized" (Image J imaging software, NIH, Bethesda, MD).

Quantification of colocalization of α subunit-IR within primary afferent terminals was likewise performed by confocal laser scanning microscopy in sections from five adult mice. The analysis was done in high magnification images acquired at the Nyquist rate (56 nm/pixel; 150 nm spacing). To minimize false-positive results, additional criteria were applied: (a) The α subunit staining is completely inside the axon terminal staining; (b) the area of colocalization >20 pixels (>0.063 μm^2); (c) co-

localization was visible in three consecutive confocal sections. The data were acquired in six sections per animal and analyzed statistically using non-parametric tests (Kruskal–Wallis followed by Dunn's multiple comparison test; Prism, GraphPad Software, San Diego, CA, USA). All files were randomized and individual terminals were identified as isolated objects and counted automatically (Imaris; Bitplane).

Results

Differential distribution of $GABA_AR$ α subunits in mouse spinal dorsal horn

The distribution of α subunit variants was examined in transverse sections of the lumbar spinal cord using immunoperoxidase staining with subunit-specific antibodies. In order to visually enhance the differences in staining intensity across layers, images are displayed in false-colors ranging from dark blue for weak signals to red, pink, orange, yellow and white for maximal intensity (Fig. 1A-E). For each antibody, signals were normalized to display the strongest signals in white, except for the α4 subunit, where only background was detected. Higher magnification images of the dorsal horn are also shown in color photomicrographs of immunoperoxidase staining (Fig. 1F-I). At the macroscopic level, α1, α2, α3, and α5 subunit immunoreactivity showed a widespread but differential laminar distribution pattern, whereas the α4 subunit was not detectable although a strong signal was observed in specific forebrain regions (e.g., thalamus) using the same staining conditions (not shown). As described previously in rat (Bohlhalter et al., 1996), IR was restricted to the grey matter except for dendrites extending radially into the white matter. In lamina I, mainly the α2 and α3 subunits were detected, along with a few α1 subunit-positive cells. Staining for the α2 and α3 subunits was most intense in lamina II, along with a moderate α5 subunit-IR. In addition, the α1 subunit was detected in the innermost lamina II. In lamina III, all four subunit variants were present with a peak staining intensity for the α3 and α5 subunit, a moderate α2 subunit staining and weak α1 subunit-IR. The latter was stronger in laminae IV-V in which α2, α3, and α5 subunit-IR was also detected at moderate levels. A distinct gradient of intensity was evident medio-laterally, culminating with intense staining of lamina X, around the central canal, notably for the α1, α2, and α3 subunit. In summary, a roughly complementary distribution pattern was observed between the α1 and α2 subunit in laminae I-III, whereas the α3 and α5 subunit largely overlapped in lamina III. The overall strong IR of these four α subunits (which all contribute to assembly of diazepam-sensitive $GABA_AR$) in the superficial dorsal horn compared with the intermediate zone and ventral horn underscores the relevance of $GABA_AR$ for processing of nociceptive inputs in the spinal cord.

Neuron-specific expression of α subunit variants

To determine whether these differential distribution patterns reflect possible neural circuit specificity, we investigated the distribution of the four α subunit variants in neurons identified by their transmitter phenotype (glutamatergic, GABAergic, glycinergic) using transgenic mice expressing vGluT2-eGFP, GlyT2-eGFP, and GAD67-eGFP, respectively. To unambiguously determine the laminar distribution of these neuronal populations, CGRP was used as a marker to differentiate lamina I from lamina IIo (Fig. 2A) and IB4 for separating lamina IIo from lamina IIi. In preliminary experiments, we confirmed that IB4 labeling is limited to the outer part of lamina IIi (Fig. 2A), using PKCγ as a specific marker of lamina II-III boundary (Neumann et al., 2008). Figure 2B-C illustrates in fluorescence microscopy the three classes of interneurons with respect to IB4 labeling. Both vGluT2-eGFP- and GAD67-eGFP-positive neurons were distributed evenly in laminae IIo, IIi and III, whereas GlyT2-eGFP-positive neurons were mainly located in laminae III-IV and scarcely in lamina IIo at the border with lamina I.

We analyzed systematically each neuronal population to determine which proportion of them was immunopositive for the α2/α3 subunits (most abundant in layer II) and α1/α5 subunits (most abundant in layers III-IV). Data are pooled from 2-3 mice per genotype, with ≈50 randomly selected eGFP-positive neurons per mouse being assessed in each lamina for colocalization with α subunit-IR. This analysis was performed in perfusion-fixed tissue, in which eGFP signals are optimally preserved, notably in thin dendritic profiles. Under these conditions, staining was rather uniform and diffuse in the neuropil and it was not possible to distinguish postsynaptic from extrasynaptic $GABA_AR$ subunit staining (Fritschy et al., 1998). Double-labeled dendrites were also seen, but were not quantified, as they could not be allocated to identified cells. Therefore, quantitative analysis was restricted to double-labeled cell bodies. Further, we could not determine whether multiple α subunit variants were present in the same cell; however, this information is inferred when the total percentage of colocalization exceeds 100%. Representative examples of each colocalization pattern are shown in Figure 2D-O and the quantitative results are provided in Figure 3A-C.

vGluT2-eGFP-positive glutamatergic neurons

Considerable laminar specificity was observed in the distribution of α subunit variants in vGluT2-eGFP-positive cells, with α2/α3 subunit-IR being each present in about 40% of cells in lamina IIo, along with the α5 subunit in a small fraction of cells, whereas in lamina IIi, almost all eGFP-positive cells were double-labeled for the α3 subunit and >50% for the α2 subunit. In lamina III, vGluT2-eGFP-positive cells likely expressed more than one α subunit variant, the proportion of co-localization ranging from 25% for the α2 subunit to 70% for the α3 subunit, with a significant contribution of α1 and α5 subunit, as well (Fig. 3A). These percentages of colocalization well matched the fraction of dendritic profiles immunoreactive for each subunit in the various laminae (Fig. 2D, G, J, M), suggesting overall a somato-dendritic localization of $GABA_AR$ in glutamatergic dorsal horn interneurons and a major influence of α3-$GABA_AR$, notably in lamina IIi.

GAD67-eGFP-positive GABAergic interneurons

In contrast to the pattern shown by excitatory interneurons, only around 5% GAD67-eGFP-positive cells in lamina IIo had α2 subunit-IR, along with 72% of cells in lamina IIi. Besides, α2 subunit-IR was present in around 40% cells located at the lamina IIi-III border. α3 subunit-IR was observed in 37 and 85% of GAD67-eGFP-positive cells in lamina IIo and IIi respectively. Therefore, in lamina IIi most of these cells have both α2- and α3-$GABA_AR$. In lamina III, α3 subunit-IR was observed in 50% of GAD67-eGFP-positive cells and the α5 subunit-IR in 60% of them, suggesting possible co-occurrence of these subunits in individual neurons. As seen for vGluT2-eGFP neurons, a large fraction of GAD67-eGFP-positive dendritic profiles were double-labeled for the α2 or α3 subunits in these experiments (Fig. 2E, H, K, N), suggesting that GABAergic synapses are distributed onto both dendritic and perisomatic areas.

GlyT2-eGFP-positive glycinergic neurons

GlyT2-eGFP-positive glycinergic cell somata were strikingly rare lamina II (absent in lamina IIi) and were more frequently detected in laminae III-V. The majority of the few cells in lamina IIo contained both α2 and α3 subunits and almost all GlyT2-eGFP-positive neurons in deeper laminae were positive for the α3 subunit-IR. The α1

and α5 subunits were detected in a few fluorescent cells of lamina IIo, (around 10-15%) and about 25% in lamina III (Fig. 3C). The dendrites of glycinergic neurons were only occasionally labeled for a $GABA_AR$ subunit (Fig. 2F, I, L, O), suggesting a concentration of inputs in the perisomatic area.

$GABA_AR$ subunit distribution in primary afferent terminals

A large fraction of the neuropil staining seen for the various α subunit variants was not colocalized with dendritic profiles. Therefore, we investigated whether this pattern reflects the presence of $GABA_AR$ in primary afferent fiber terminals. CGRP and IB4 labeling were used to reveal peptidergic and non-peptidergic C-fibers, respectively. The specificity of these markers was confirmed by double labeling with antibodies against substance P to label peptidergic fibers and against the extracellular matrix proteoglycan versican 2, an identified IB4-binding glycoconjugate (Bogen et al., 2005; Gibbins et al., 1987) (data not shown). Myelinated fibers in the dorsal horn were labeled by transganglionic tracing of cholera toxin subunit B (CTB) injected into the sciatic nerve (Fig. 4A), as well as by immunofluorescence against vGluT1 (data not shown) (Todd et al., 2003). Triple labeling experiments performed using antibodies against CGRP and CTB along with either anti-PKCγ or fluorescently-tagged IB4 to confirm the distinct laminar distribution of these markers in primary afferent terminals in the dorsal horn (Fig. 4B-B'). CGRP, IB4 and CTB were then analyzed separately for colocalization of α subunit-immunofluorescence.

For all α subunit variants, we observed at high magnification that the punctate staining of the neuropil was partially colocalized with each of the three markers of primary afferents. For quantification, colocalization was defined by an intensity threshold algorithm using stringent criteria (see Materials and Methods). It is of note, however, that the region containing the presynaptic active zone could not be identified in primary afferent profiles, because neither vGluT1 nor vGluT2 are detectable in the terminals of C-fibers. Quantitative results are presented in Fig. 3D-E, representing average data (± SD) from 5 mice per group.

In lamina IIo, a large fraction of CGRP-positive profiles, 28% and 59%, respectively, contained α2 and α3 subunit-IR (Fig. 4A-J). Likewise, 43% and 46% of IB4-labeled profiles in lamina IIi, and 18% and 21% of CTB-positive profiles in lamina III were colocalized with α2 and α3 subunit-IR (Fig. 3D). The density of puncta

immunoreactive for each subunit was also analyzed (Fig. 3E). Lamina IIo showed a density of 38 and 85 α2 and α3 subunit puncta, respectively, colocalized with CGRP-IR per 1000 μm^2. In lamina IIi and III, 56 α2 subunit and 58 α3 subunit puncta were co-localized with IB4 labeling, and 28 and 40 with CTB-IR.

The α1 subunit was scarcely detected in CGRP- and IB4-positive profiles in lamina II, suggesting that it is not associated with C-fibers (Fig. 3D, E), in spite of the moderate staining intensity for this subunit in lamina IIi (Fig. 1). In contrast, α1 subunit-IR was detected in 13% CTB-positive profiles in lamina III, representing 15 puncta per 1000 μm^2 (Fig. 3E).

The α5 subunit showed high colocalization rate with CGRP-positive profiles (15%), but less than 3% with IB4-labeled profiles (Fig. 3D). The highest colocalization rate for the α5 subunit was detected in CTB-IR profiles, reaching 44%. The density analysis showed 17, 1 and 22 puncta per 1000 μm^2 in CGRP, IB4 and CTB staining, respectively (Fig. 3E).

These data reveal a clear specificity in the occurrence of $GABA_AR$ subtype markers in primary afferent terminals of the superficial dorsal horn, with peptidergic and non-peptidergic fibers being associated mainly with the α3 and α2 subunits; in addition, some peptidergic fibers contain α5-$GABA_AR$, whereas CTB-positive profiles, representing myelinated fiber terminals, are associated with the four diazepam-sensitive α subunit variants.

Identification of putative GABAergic synapses on primary afferent terminals

The presence of $GABA_AR$ in primary afferent suggests a major role for filtering incoming nociceptive sensory information. To determine whether this function is assumed by GABAergic synapses, we carried our analysis further to visualize postsynaptic α2 and α3 subunit clusters, apposed to presumptive presynaptic terminals identified by staining for vesicular inhibitory transporter (VIAAT) and colocalized with gephyrin within labeled primary afferent terminals. These two markers allow for a selective discrimination of pre- and postsynaptic components of inhibitory synapses. These experiments were performed in weakly fixed tissue to maximize the detection of postsynaptic proteins (see Materials and Methods). As a prerequisite, double immunofluorescence experiments showed a systematic apposition of VIAAT-positive profile to gephyrin clusters, indicating the presence of

postsynaptic $GABA_AR$ (Fig. 5A). While a large fraction of these gephyrin clusters likely are located postsynaptically in dendrites and neuronal somata, confocal laser scanning microscopy analysis showed gephyrin clusters also in a subset of peptidergic and non-peptidergic C-fibers in laminae I-II, as well as myelinated fibers in laminae III-V (data not shown). A substantial fraction (≈30%) of these gephyrin clusters was colocalized with the α2 and α3 subunit-IR.

Quadruple immunohistochemistry was performed eventually with the combination of VIAAT, gephyrin, a primary afferent marker and α2 or α3 subunit antibody (Fig. 5C-G), using primary antibodies raised in different species. We detected gephyrin along with either α2 or α3 subunit-IR in individual primary afferent terminal profiles from all three classes apposed to a VIAAT-profile, suggestive of a synaptic contact. A representative example is shown for the α3 subunit in IB4-positive terminals (Fig. 5C-G). These observations provide a proof-of-principle for the presence of α2- and α3-$GABA_AR$ associated with gephyrin in axo-axonic synapses onto primary afferent terminals.

Gephyrin mRNA and protein expression in DRG neurons

To validate the presence of gephyrin-IR inside primary afferent terminals, we verified that gephyrin is expressed in the DRG using qRT-PCR and Western blotting. Thus, qPCR analysis using Taqman assays using β-actin as reference confirmed the detection of gephyrin mRNA in DRG lysate. Relative to GAPDH, gephyrin mRNA copy number detected was 2.25±1.1%. Likewise, Western blot analysis of gephyrin in crude extracts of lumbar DRG and adult mouse brain homogenate as control confirmed the presence of gephyrin protein in both preparations, detected as a band with apparent molecular weight of 95 kDa (Fig. 5B).

Discussion

The present results demonstrate that the differential laminar distribution of $GABA_AR$ subtypes in the dorsal horn, distinguished by their α subunit variant, corresponds to a complex cell-specific and primary afferent-specific expression pattern. These findings provide a framework to investigate how $GABA_AR$ subtypes differentially regulate sensory processing and pain by controlling the activity of different neuronal networks. The highest degree of $GABA_AR$ heterogeneity occurs in lamina III, suggesting the existence with multiple parallel circuits controlled by distinct $GABA_AR$, as well as convergence of circuits impinging onto spinal cord neurons that express multiple $GABA_AR$ subtypes. $GABA_AR$ in glutamatergic primary afferents and neurons likely mediate inhibition by controlling transmitter release and postsynaptic excitation, respectively. In contrast, $GABA_A$-mediated inhibition of GABAergic interneurons might be of particular relevance for disinhibition of specific neuronal circuits (Labrakakis et al., 2009). Pharmacologically, $GABA_AR$ heterogeneity in spinal cord circuits is of immediate relevance for the treatment of distinct pain modalities with subtype-selective ligands.

Methodological considerations

Compelling evidence from morphological, functional, and pharmacological studies indicates that the six α subunit variants correspond to distinct $GABA_AR$ subtypes (Fritschy and Brunig, 2003; Olsen and Sieghart, 2008; Rudolph et al., 2001; Sieghart, 2006) and, therefore, can be used as subtype markers for immunohistochemistry. Importantly, because an α subunit is required for assembly and cell surface expression of most $GABA_AR$ (Kralic et al., 2006; Panzanelli et al., 2011; Studer et al., 2006; Sur et al., 2001; Vicini et al., 2001), their detection by immunofluorescence implies the presence of β and γ subunit variants in the same cells. However, one cannot distinguish in neurons expressing two different α subunit variants whether they are part of the same receptor complex or correspond to two receptor subtypes intermingled within the same synapse (Panzanelli et al., 2011). Therefore, it is not possible to define morphologically or functionally all neuronal circuits controlled by a given $GABA_AR$ subtype.

Despite the importance of inhibitory neurotransmission for nociception, there is only limited information available on the cellular and subcellular distribution of $GABA_AR$

in the spinal cord dorsal horn, in part due to technical limitations. First, the small size of neurons and thin diameter of their dendrites, combined with their high packing density and the presence of numerous immunopositive primary afferent terminals, makes it very difficult to assign an immunopositive profile to an identified cell. In particular, the distinction between postsynaptic and extrasynaptic $GABA_AR$, which in brain sections can be achieved in mildly-fixed tissue (Schneider Gasser et al., 2006), is obscured in the spinal cord by the extensive labeling of primary afferent terminals. Furthermore, using transgenic mouse lines, which express eGFP in a neurotransmitter-specific manner, it is not certain that all neurons using this neurotransmitter are labeled. In particular, GABAergic neurons expressing only GAD65-only are not visible in GAD67-eGFP mice (Tamamaki et al., 2003; Wang et al., 2009). Likewise, while vGluT2-eGFP is expressed selectively in glutamatergic neurons, it is not known which fraction of these cells express this marker. A further limitation of the method is that it did allow us to quantify double labeled cells only on the basis of somatic, but not dendritic labeling.

With regard to primary afferent terminals, colocalization analysis is limited by the resolution of confocal microscopy, in particular along the z-axis. We have taken a conservative approach based on stringent criteria for assessing the presence of α subunit-IR inside labeled primary afferent terminals (see Materials and Methods). The validity of this approach was confirmed recently by the analysis of the α2 subunit in mice carrying a conditional deletion of *Gabra2* selectively in nociceptors (Witschi et al., 2011). However, in the absence of a marker of the presynaptic active zone or presynaptic vesicles in primary afferent terminals, it was not possible to determine the localization of α subunit-IR relative to these structures. To overcome this problem, we attempted to determine the presence of axo-axonic GABAergic synapses onto primary afferent terminals, using VIAAT and gephyrin as markers. This approach provided strong evidence that such synapses exist in principle, in line with ultrastructural evidence for the presence of axo-axonic GABAergic synapses on primary afferent glomeruli (Ribeiro-da-Silva and Coimbra, 1982; Ribeiro-da-Silva et al., 1985; Todd, 1996). However, although our approach did not allow a reliable quantification of their abundance, only a minority of profiles immunopositive for CGRP or IB4, as well as those labeled with CTB appeared to contain a gephyrin cluster. Such negative results may not be fully conclusive, especially when

presynaptic terminals cannot be distinguished from preterminal axons, but they still suggest that in the majority of cases, $GABA_AR$ in C-fiber terminals or in myelinated nociceptor terminals are activated by GABA spillover in the extracellular space, rather than by phasic GABA release.

Organization of $GABA_AR$ subtypes in intrinsic spinal dorsal horn neurons

Despite these limitations, our results clearly show that the four α subunit variants contributing to the assembly of diazepam-sensitive $GABA_AR$ (Rudolph and Mohler, 2006) are present in the spinal cord dorsal horn with distinct laminar, cellular and subcellular distributions. Therefore, modulation of distinct pain modalities and/or functional alterations of GABAergic inhibition in specific neuronal circuits in the dorsal horn can be expected from our results in models of chronic pain. Moreover, the failure to detect the α4 subunit indicates that this diazepam-insensitive $GABA_AR$ subtypes likely plays only a minor role in the spinal cord.

We observed a distinct laminar distribution of the α1, α2, α3, and α5 subunit-IR with considerable overlap within individual laminae. These findings imply that some neurons express multiple α subunit variants (notably α2/α3 in lamina IIo), whereas others have a single α subunit (notably in lamina IIi and III). A striking overall feature is the prominent α2 subunit staining in lamina II – also observed in the rat (Bohlhalter et al., 1996), which contrasts with the lack of α2 subunit mRNA expression reported in the dorsal horn (Persohn et al., 1991; 1992; Wisden et al., 1991). However, our present data demonstrate the presence of eGFP-positive cells immunoreactive for the α2 and α3 subunit in lamina II, with a predominance of the α3 subunit-IR (Knabl et al., 2008). Therefore, in situ hybridization with radiolabeled oligonucleotides might lack sensitivity for detecting α2 subunit mRNA in lamina II neurons. Nevertheless, most α2 subunit-IR was located in the neuropil, presumably on primary afferent terminals and possibly also on dendrites from neurons located in deeper layers.

Glutamatergic neurons identified by vGluT2-eGFP expression likely express different α subunits in lamina IIo (either α2 or α3 subunit) and III (α1, α5, α3), and both α2/α3 subunits in lamina IIi, providing a clear example of differential control by distinct $GABA_AR$ subtypes. The implications of such observations are that subtype-selective $GABA_AR$ ligands would produce distinct effects on glutamatergic neuronal

circuits in these three laminae, which are innervated by different subpopulations of primary afferent terminals.

It is most remarkable that at least 40% GAD67-eGFP neurons apparently lack labeling for any $GABA_AR$ subunit on their soma in lamina IIo (Figure 3), despite the abundant α2 and α3 subunit-IR in this sublamina, suggesting that these GABAergic neurons receive only limited perisomatic GABAergic inhibitory input. As noted above, our study provides no data on cells selectively expressing GAD65 in the spinal cord. Such cells are rare in the forebrain, where GAD67-eGFP labels the vast majority of GABAergic cells (Tamamaki et al., 2003). In case of spinal cord, GAD65 has been shown to be expressed in a specific GABAergic interneuronal population, which is specifically presynaptic to the proprioceptive terminals (Betley et al., 2009; Hughes et al., 2005).

Glycinergic neurons, which are rare in lamina IIo but abundant in lamina III, widely express the α3 subunit, along with either α2 in lamina IIo, or, in equal proportion α1, α2 or α5 subunit in lamina III. These features provide a substrate for possible cross-talk between the two inhibitory systems.

Functional organization of $GABA_A$ receptor subtypes on primary afferent terminals

Primary afferent depolarization is well known to occur in spinal cord, and $GABA_AR$ have been shown long ago to mediate the inhibition of potassium-stimulated CGRP release in spinal cord tissue (Bourgoin et al., 1992). Overall, the presence of presynaptic $GABA_AR$ in major brain regions, including cerebral cortex, hippocampus, and cerebellum, is undisputed (Hutcheon et al., 2000; Trigo et al., 2010; Vautrin et al., 1994). However, immunohistochemical studies have largely failed so far to reveal their distribution and subunit composition. Therefore, the spinal cord appears to be unique for the prominent labeling of multiple $GABA_AR$ subunits in terminals of both myelinated and non-myelinated sensory afferents. The present study confirms our previous observations (Knabl et al., 2008; Witschi et al., 2011) and provides proof-of-principle evidence that these $GABA_AR$ correspond, at least in part, to axo-axonic synapses, with a postsynaptic density containing the scaffolding protein gephyrin. Moreover, our results show an IR pattern of the various α subunit variants compatible with a complementary distribution (one $GABA_AR$ subtype per afferent terminal); C-fiber terminals containing either α2- or α3-$GABA_AR$, whereas myelinated terminals

in layer III containing in roughly equal proportion one of the four diazepam-sensitive $GABA_AR$ subtypes. These results are compatible with the notion that distinct $GABA_AR$ subtypes modulate the function of primary afferent carrying specific pain modalities and/or being differentially involved in various forms of chronic pain (Zeilhofer et al., 2012a; Zeilhofer et al., 2009). Moreover, while diazepam can be expected to potentiate the action of $GABA_AR$ in primary afferents, subtype-selective ligands would potentially exert more selective effects.

There is increasing evidence for the existence of segregated circuits mediating specific pain-related modalities in the dorsal horn (Neumann et al., 2008; Todd, 2010; Zylka et al., 2005). For instance, a differential distribution of μ- and δ-opioid receptors in subsets of peptidergic and non-peptidergic nociceptors, respectively, regulating distinct pain modalities (heat and mechanical pain) has been reported (Scherrer et al., 2009). TRPV1 receptors, critical for the development of thermal hyperalgesia, also have been found to be restricted to a subset of peptidergic nociceptors in lamina IIo (Cavanaugh et al., 2011) whereas TRPV2, which is expressed non-peptidergic and myelinated nociceptors terminating in lamina IIi and in deeper laminae was conclusively shown to be dispensable for progression of thermal hyperalgesia (Park et al., 2011). In line with these observations, we have shown that mice lacking α2-$GABA_AR$ specifically in primary nociceptors (sns-$\alpha2^{-/-}$ mice) exhibit reduced potentiation of dorsal root potentials and impaired thermal and mechanical anti-hyperalgesia by diazepam in a model of inflammatory pain (Witschi et al., 2011).

The role of α3-$GABA_AR$ in lamina II neurons and primary afferents for the control of hyperalgesia is less well established. They contribute in part to thermal and mechanical hyperalgesia in models of inflammatory and neuropathic pain, possibly along with a contribution by α5-$GABA_AR$ (Knabl et al., 2008; Munro et al., 2011). Finally, based on their distribution on myelinated fibers and lamina III neurons, α5-$GABA_AR$ could have a major role in regulation of allodynia.

The relevance of our finding possibility extends beyond pain control, notably if primary afferent depolarization were involved in other pathological sensory modalities, such as itch. Both C-fibers and Aδ-fibers have been shown to convey this sensation elicited by histamine (Andrew and Craig, 2001; Potenzieri and Undem, 2012; Schmelz et al., 1997). In addition, decreased inhibitory synaptic input to

nociceptive terminals in lamina I-II elicits itch (Ross et al., 2010), in line with our findings.

Conclusions

Collectively, the present results show that $GABA_AR$ distribution in the primary afferent terminals and intrinsic dorsal horn neurons of the dorsal horn allows for multiple, circuit-specific modes of regulation of neuronal networks. This conclusion confirms previous evidence for a differential contribution of α2- and α2/α3/α5-$GABA_AR$ for thermal and mechanical anti-hyperalgesia, respectively (Knabl et al., 2008). The likely existence of parallel and serial connections involving GABAergic neurons allows for both inhibition and disinhibition in a pain modality-specific manner. This organization pattern of $GABA_ARs$ in the adult spinal cord might be altered morphologically and functionally in chronic pain conditions. Identifying these alterations in mouse models of chronic inflammatory and neuropathic pain, will facilitate the design of novel therapeutic avenues based on $GABA_AR$ subtype-selective ligands.

Acknowledgements

We are grateful to Dr. Yuchio Yanagawa (Gunma University Graduate School of Medicine, Maebashi, Japan) for providing GAD67-eGFP mice and Dr. Dietmar Benke, Louis Scheurer, and Isabelle Camenisch for help with biochemical experiments, real time PCR and mouse genotyping. The authors have no competing interests to declare.

References

Andrew D, Craig AD. 2001. Spinothalamic lamina I neurones selectively responsive to cutaneous warming in cats. J Physiol 537:489-495.

Bellocchio EE, Reimer RJ, Fremeau RT, Jr., Edwards RH. 2000. Uptake of glutamate into synaptic vesicles by an inorganic phosphate transporter. Science 289:957-960.

Bencsits E, Ebert V, Tretter V, Sieghart W. 1999. A significant part of native γ-aminobutyric $acid_A$ receptors containing α4 subunits do not contain γ or δ subunits. J Biol Chem 274:19613-19616.

Betley JN, Wright CV, Kawaguchi Y, Erdelyi F, Szabo G, Jessell TM, Kaltschmidt JA. 2009. Stringent specificity in the construction of a GABAergic presynaptic inhibitory circuit. Cell 139:161-174.

Bogen O, Dreger M, Gillen C, Schroder W, Hucho F. 2005. Identification of versican as an isolectin B4-binding glycoprotein from mammalian spinal cord tissue. FEBS J 272:1090-1102.

Bohlhalter S, Weinmann O, Mohler H, Fritschy JM. 1996. Laminar compartmentalization of $GABA_A$-receptor subtypes in the spinal cord. J Neurosci 16:283-297.

Bourgoin S, Pohl M, Benoliel JJ, Mauborgne A, Collin E, Hamon M, Cesselin F. 1992. γ-Aminobutyric acid, through $GABA_A$ receptors, inhibits the potassium-stimulated release of calcitonin gene-related peptide- but not that of substance P-like material from rat spinal cord slices. Brain Res 583:344-348.

Brünig I, Suter A, Knuesel I, Luscher B, Fritschy JM. 2002. GABAergic presynaptic terminals are required for postsynaptic clustering of dystrophin, but not of $GABA_A$ receptors and gephyrin. J Neurosci 22:4805-4813.

Cavanaugh DJ, Chesler AT, Bráz JM, Shah NM, Julius D, Basbaum AI. 2011. Restriction of transient receptor potential vanilloid-1 to the peptidergic subset of primary afferent neurons follows its developmental downregulation in nonpeptidergic neurons. J Neurosci 31:10119-10127.

Chang HM, Wei IH, Tseng CY, Lue JH, Wen CY, Shieh JY. 2004. Differential expression of calcitonin gene-related peptide (CGRP) and choline acetyltransferase (ChAT) in the axotomized motoneurons of normoxic and hypoxic rats. J Chem Neuroanat 28:239-251.

Clavier N, Lombard MC, Besson JM. 1992. Benzodiazepines and pain: effects of midazolam on the activities of nociceptive non-specific dorsal horn neurons in the rat spinal cord. Pain 48:61-71.

Dirmeier M, Capellino S, Schubert T, Angele P, Anders S, Straub RH. 2008. Lower density of synovial nerve fibres positive for calcitonin gene-related peptide relative to substance P in rheumatoid arthritis but not in osteoarthritis. Rheumatol 47:36-40.

Eaton MJ, Martinez MA, Karmally S. 1999. A single intrathecal injection of GABA permanently reverses neuropathic pain after nerve injury. Brain Res 835:334-339.

Encinas JM, Vaahtokari A, Enikolopov G. 2006. Fluoxetine targets early progenitor cells in the adult brain. Proc Natl Acad Sci U S A 103:8233-8238.

Fremeau RT, Voglmaier S, Seal RP, Edwards RH. 2004. VGLUTs define subsets of excitatory neurons and suggest novel roles for glutamate. Trends Neurosci 27:98-103.

Fritschy JM, Benke D, Johnson DK, Mohler H, Rudolph U. 1997. $GABA_A$-receptor α-subunit is an essential prerequisite for receptor formation in vivo. Neurosci 81:1043-1053.

Fritschy JM, Brunig I. 2003. Formation and plasticity of GABAergic synapses: physiological mechanisms and pathophysiological implications. Pharmacol Ther 98:299-323.

Fritschy JM, Panzanelli P, Kralic JE, Vogt KE, Sassoè-Pognetto M. 2006. Differential dependence of axo-dendritic and axo-somatic GABAergic synapses on $GABA_A$ receptors containing the α1 subunit in Purkinje cells. J Neurosci 26:3245-3255.

Fritschy JM, Weinmann O, Wenzel A, Benke D. 1998. Synapse-specific localization of NMDA and $GABA_A$ receptor subunits revealed by antigen-retrieval immunohistochemistry. J Comp Neurol 390:194-210.

Fujiyama F, Furuta T, Kaneko T. 2001. Immunocytochemical localization of candidates for vesicular glutamate transporters in the rat cerebral cortex. J Comp Neurol 435:379-387.

Gibbins IL, Wattchow D, Coventry B. 1987. Two immunohistochemically identified populations of calcitonin gene-related peptide (CGRP)-immunoreactive axons in human skin. Brain Res 414:143-148.

Gong S, Zheng C, Doughty ML, Losos K, Didkovsky N, Schambra UB, Nowak NJ, Joyner A, Leblanc G, Hatten ME, Heintz N. 2003. A gene expression atlas of the central nervous system based on bacterial artificial chromosomes. Nature 425:917-925.

Hughes DI, Mackie M, Nagy GG, Riddell JS, Maxwell DJ, Szabó G, Erdélyi F, Veress G, Szucs P, Antal M, Todd AJ. 2005. P boutons in lamina IX of the rodent spinal cord express high levels of glutamic acid decarboxylase-65 and originate from cells in deep medial dorsal horn. Proc Natl Acad Sci U S A 102:9038-9043.

Hunt SP, Mantyh PW. 2001. The molecular dynamics of pain control. Nature Rev Neurosci 2:83-91.

Hutcheon B, Brown LA, Poulter MO. 2000. Digital analysis of light microscope immunofluorescence: high-resolution co-localization of synaptic proteins in cultured neurons. J Neurosci Met 96:1-9.

Jasmin L, Rabkin SD, Granato A, Boudah A, Ohara PT. 2003. Analgesia and hyperalgesia from GABA-mediated modulation of the cerebral cortex. Nature 424:316-320.

Knabl J, Witschi R, Hosl K, Reinold H, Zeilhofer UB, Ahmadi S, Brockhaus J, Sergejeva M, Hess A, Brune K, Fritschy JM, Rudolph U, Mohler H, Zeilhofer HU. 2008. Reversal of pathological pain through specific spinal $GABA_A$ receptor subtypes. Nature 451:330-334.

Kralic JE, Sidler C, Parpan F, Homanics GE, Morrow AL, Fritschy JM. 2006. Compensatory alteration of inhibitory synaptic circuits in cerebellum and thalamus of γ-aminobutyric acid type A receptor α1 subunit knockout mice. J Comp Neurol 495:408-421.

Labrakakis C, Lorenzo L, Bories C, Ribeiro-da-Silva A, De Koninck Y. 2009. Inhibitory coupling between inhibitory interneurons in the spinal cord dorsal horn. Mol Pain 5:24:1-8.

Ma W, Saunders PA, Somogyi R, Poulter MO, Barker JL. 1993. Ontogeny of $GABA_A$ receptor subunit mRNAs in rat spinal cord and dorsal root ganglia. J Comp Neurol 338:337-359.

Melzack, R, Wall PD. 1965. Pain mechanisms: A new theory. Science 150:971-978.

Möhler H. 2006. $GABA_A$ receptor diversity and pharmacology. Cell Tissue Res 326:505-516.

Munro G, Erichsen HK, Rae MG, Mirza NR. 2011. A question of balance--positive versus negative allosteric modulation of $GABA_A$ receptor subtypes as a driver of analgesic efficacy in rat models of inflammatory and neuropathic pain. Neuropharmacol 61.

Nahmani M, Erisir A. 2005. VGluT2 immunochemistry identifes thalamocortical terminals in layer 4 of adult and developing visual cortex. J Comp Neurol 484:458-473.

Neumann S, Braz JM, Skinner K, Llewellyn-Smith IJ, Basbaum AI. 2008. Innocuous, not noxious, input activates PKCgamma interneurons of the spinal dorsal horn via myelinated afferent fibers. J Neurosci 28:7936-7944.

Olsen RW, Sieghart W. 2008. International Union of Pharmacology. LXX. Subtypes of γ-aminobutyric $acid_A$ receptors: classification on the basis of subunit composition, pharmacology, and function. Update. Pharmacol Rev 60:243.

Panzanelli P, Bardy C, Nissant A, Pallotto M, Sassoè-Pognetto M, Lledo PM, Fritschy JM. 2009. Early synapse formation in developing interneurons of the adult olfactory bulb. J Neurosci 29:15039-15052.

Panzanelli P, Gunn BG, Schlatter MC, Benke D, Tyagarajan SK, Scheiffele P, Belelli D, Lambert JJ, Rudolph U, Fritschy JM. 2011. Distinct mechanisms regulate $GABA_A$ receptor and gephyrin clustering at perisomatic and axo-axonic synapses on CA1 pyramidal cells. J Physiol 589:4959-4980.

Park U, Vastani N, Guan Y, Raja SN, Koltzenburg M, Caterina MJ. 2011. TRP vanilloid 2 knock-out mice are susceptible to perinatal lethality but display normal thermal and mechanical nociception. J Neurosci 31:11425-11436.

Peng Z, Hauer B, Mihalek RM, Homanics GE, Sieghart W, Olsen RW, Houser CR. 2002. $GABA_A$ receptor changes in δ subunit-deficient mice: altered expression of α4 and γ2 subunits in the forebrain. J Comp Neurol 446:179-197.

Persohn E, Malherbe P, Richards JG. 1991. In situ hybridization histochemistry reveals a diversity of $GABA_A$ receptor subunit mRNAs in neurons of the rat spinal cord and dorsal root ganglia. Neurosci 42:497-507.

Persohn E, Malherbe P, Richards JG. 1992. Comparative molecular neuroanatomy of cloned $GABA_A$ receptor subunits in the rat CNS. J Comp Neurol 326:193-216.

Pfeiffer F, Simler R, Grenningloh G, Betz H. 1984. Monoclonal antibodies and peptide mapping reveal structural similarities between the subunits of the glycine receptor of rat spinal cord. Proc Natl Acad Sci U S A 81:7224-7227.

Potenzieri C, Undem BJ. 2012. Basic mechanisms of itch. Clin Exp Allergy 42:8-19.

Rexed B. 1952. The cytoarchitectonic organization of the spinal cord in the cat. J Comp Neurol 96:415-495.

Ribeiro-da-Silva A, Coimbra A. 1982. Two types of synaptic glomeruli and their distribution in laminae I-III of the rat spinal cord. J Comp Neurol 209:176-186.

Ribeiro-da-Silva A, Pignatelli D, Coimbra A. 1985. Synaptic architecture of glomeruli in superficial dorsal horn of rat spinal cord, as shown in serial reconstructions. J Neurocytol 14:203-220.

Roberts LA, Beyer C, Komisaruk BR. 1986. Nociceptive responses to altered GABAergic activity at the spinal cord. Life Sci 39:1667-1674.

Ross SE, Mardinly AR, McCord AE, Zurawski J, Cohen S, Jung C, Hu L, Mok SI, Shah A, Savner EM, Tolias C, Corfas R, Chen S, Inquimbert P, Xu Y,

McInnes RR, Rice FL, Corfas G, Ma Q, Woolf CJ, Greenberg ME. 2010. Loss of inhibitory interneurons in the dorsal spinal cord and elevated itch in Bhlhb5 mutant mice. Neuron 65:886-898.

Rudolph U, Crestani F, Mohler H. 2001. $GABA_A$ receptor subtypes: dissecting their pharmacological functions. Trends Pharmacol Sci 22:188-194.

Rudolph U, Mohler H. 2006. GABA-based therapeutic approaches: $GABA_A$ receptor subtype functions. Curr Opin Pharmacol 6:18-23.

Sassoè-Pognetto M, Panzanelli P, Sieghart W, Fritschy JM. 2000. Co-localization of multiple $GABA_A$ receptor subtypes with gephyrin at postsynaptic sites. J Comp Neurol 420:481-498.

Sastry BR. 1980. Potentiation of presynaptic inhibition of nociceptive pathways as a mechanism for analgesia. Can J Physiol Pharmacol 58:97-101.

Scherrer G, Imamachi N, Cao YQ, Contet C, Mennicken F, O'Donnell D, Kieffer BL, Basbaum AI. 2009. Dissociation of the opioid receptor mechanisms that control mechanical and heat pain. Cell 137:1148-1159.

Schmalfeldt M, Dours-Zimmermann MT, Winterhalter KH, Zimmermann DR. 1998. Versican V2 is a major extracellular matrix component of the mature bovine brain. J Biol Chem 273:15758-15764.

Schmelz M, Luz O, Averbeck B, Bickel A. 1997. Plasma extravasation and neuropeptide release in human skin as measured by intradermal microdialysis. Neurosci Lett 230:117-120.

Schneider Gasser EM, Duveau V, Prenosil GA, Fritschy JM. 2007. Reorganization of GABAergic circuits maintains $GABA_A$ receptor-mediated transmission onto CA1 interneurons in α1-subunit-null mice. Eur J Neurosci 25:3287-3304.

Schneider Gasser EM, Straub CJ, Panzanelli P, Weinmann O, Sassoe-Pognetto M, Fritschy JM. 2006. Immunofluorescence in brain sections: simultaneous detection of presynaptic and postsynaptic proteins in identified neurons. Nat Protoc 1:1887-1897.

Sieghart W. 2006. Structure, pharmacology, and function of $GABA_A$ receptor subtypes. Adv Pharmacol 54:231-263.

Studer R, von Boehmer L, Haenggi T, Schweizer C, Benke D, Rudolph U, Fritschy JM. 2006. Alteration of GABAergic synapses and gephyrin clusters in the thalamic reticular nucleus of $GABA_A$ receptor α3 subunit-null mice. Eur J Neurosci 24:1307-1315.

Sumida T, Tagami M, Ide Y, Nagase M, Sekiyama H, Hanaoka K. 1995. Intravenous midazolam suppresses noxiously evoked activity of spinal wide dynamic range neurons in cats. Anesth Analg 80:58.

Sur C, Wafford KA, Reynolds DS, Hadingham KL, Bromidge F, Macaulay A, Collinson N, O'Meara G, Howell O, Newman R, Myers J, Atack JR, Dawson GR, McKernan RM, Whiting PJ, Rosahl TW. 2001. Loss of the major $GABA_A$ receptor subtype in the brain is not lethal in mice. J Neurosci 21:3409-3418.

Tamamaki N, Yanagawa Y, Tomioka R, Miyazaki J, Obata K, Kaneko T. 2003. Green fluorescent protein expression and colocalization with calretinin, parvalbumin, and somatostatin in the GAD67-GFP knock-in mouse. J Comp Neurol 467:60-79.

Todd AJ. 1996. GABA and glycine in synaptic glomeruli of the rat spinal dorsal horn. Eur J Neurosci 8:2492-2498.

Todd AJ. 2010. Neuronal circuitry for pain processing in the dorsal horn. Nat Rev Neurosci 11:823-836.

Todd AJ, Hughes DI, Polgar E, Nagy GG, Mackie M, Ottersen OP, Maxwell DJ. 2003. The expression of vesicular glutamate transporters VGLUT1 and VGLUT2 in neurochemically defined axonal populations in the rat spinal cord with emphasis on the dorsal horn. Eur J Neurosci 17:13-27.

Trigo FF, Bouhours B, Rostaing P, Papageorgiou G, Corrie JE, Triller A, Ogden D, Marty A. 2010. Presynaptic miniature GABAergic currents in developing interneurons. Neuron 66:235-247.

Vautrin J, Schaffner AE, Barker JL. 1994. Fast presynaptic $GABA_A$ receptor-mediated Cl^- conductance in cultured rat hippocampal neurones. J Physiol 479 (Pt 1):53-63.

Vicini S, Ferguson C, Prybylowski K, Kralic J, Morrow AL, Homanics GE. 2001. $GABA_A$ receptor α1 subunit deletion prevents developmental changes of inhibitory synaptic currents in cerebellar neurons. J Neurosci 21:3009-3016.

Wang Y, Kakizaki T, Sakagami H, Saito K, Ebihara S, Kato M, Hirabayashi M, Saito Y, Furuya N, Yanagawa Y. 2009. Fluorescent labeling of both GABAergic and glycinergic neurons in vesicular GABA transporter (VGAT)-venus transgenic mouse. Neurosci 164:1031-1043.

Wieland HA, Lüddens H, Seeburg PH. 1992. A single histidine in $GABA_A$ receptors is essential for benzodiazepine agonist binding. J Biol Chem 267:1426.

Wisden W, Gundlach AL, Barnard EA, Seeburg PH, Hunt SP. 1991. Distribution of $GABA_A$ receptor subunit mRNAs in rat lumbar spinal cord. Mol Brain Res 10:179-183.

Witschi R, Punnakkal P, Paul J, Walczak JS, Cervero F, Fritschy JM, Kuner R, Keist R, Rudolph U, Zeilhofer HU. 2011. Presynaptic α2-$GABA_A$ receptors in primary afferent depolarization and spinal pain control. J Neurosci 31:8134.

Yaksh TL. 1989. Behavioral and autonomic correlates of the tactile evoked allodynia produced by spinal glycine inhibition: effects of modulatory receptor systems and excitatory amino acid antagonists. Pain 37:111-123.

Zeilhofer HU, Benke D, Yévenes GE. 2012a. Chronic pain states: pharmacological strategies to restore diminished inhibitory spinal pain control. Annu Rev Pharmacol Toxicol 52:111-133.

Zeilhofer HU, Möhler H, Di Lio A. 2009. GABAergic analgesia: new insights from mutant mice and subtype-selective agonists. Trends Pharmacol Sci 30:397-402.

Zeilhofer HU, Studler B, Arabadzisz D, Schweizer C, Ahmadi S, Layh B, Bosl MR, Fritschy JM. 2005. Glycinergic neurons expressing enhanced green fluorescent protein in bacterial artificial chromosome transgenic mice. J Comp Neurol 482:123-141.

Zeilhofer HU, Wildner H, Yévenes GE. 2012b. Fast synaptic inhibition in spinal sensory processing and pain control. Physiol Rev 92:193-235.

Zimmermann DR, Dours-Zimmermann MT, Schubert M, Bruckner-Tuderman L. 1994. Versican is expressed in the proliferating zone in the epidermis and in association with the elastic network of the dermis. J Cell Biol 124:817-825.

Zylka MJ, Rice FL, Anderson DJ. 2005. Topographically distinct epidermal nociceptive circuits revealed by axonal tracers targeted to Mrgprd. Neuron 45:17-25.

Figure legends

Figure 1

Differential distribution of $GABA_AR$ α subunit variants in adult mouse lumbar spinal cord. **A-E:** Each panel shows a color-coded photomicrograph of a coronal hemi-section processed for immunoperoxidase staining with subunit specific antibodies. The intensity of pixel was normalized using a custom-made look-up table showing the strongest signal in white and the background in dark blue, except for the α4 subunit, where only background staining was detected. Comparisons between antibodies are not relevant. Immunoreactive dendrites penetrating into the white matter are indicated with arrows. Notice the intense α2- **(B)** and α3 subunit **(C)** IR in lamina I and II, and α1 **(A)**, α3 and α5 subunit-IR **(E)** in lamina III-V, whereas α4 subunit-IR **(D)** was not detectable. In addition, the α1, α2, and α3 subunit-IR was prominent around the central canal (lamina X). **F:** Schematic representation of spinal cord laminae**. G-J**: Color photomicrographs of the dorsal horn, depicting the cellular distribution of the α1, α2, α3, and α5 subunit in the superficial laminae. Scale bars, 100 μm.

Figure 2

Layer-specific allocation of α subunit variants in identified subpopulations of eGFP-positive dorsal horn neurons. **A-C:** Images depicting vGluT2-eGFP (A-A'), GAD67-eGFP (**B**) and GlyT2-eGFP (**C**) neurons (green) in laminae I-III distinguished by IB4 (blue) labeling of non-peptidergic primary afferents, as well as PKCγ (red, panel A only). **D-O**: Double fluorescence labeling with antibodies to the α1, α2, α3, and α5 subunit (magenta) and eGFP (green), depicting colocalized voxels in white. Each image represents a stack of 13 confocal layers spaced by 0.3 μm. Each column represents a different neuronal marker; the lamina from which each image was taken is indicated in the lower right corner; neurons identified as double-labeled are shown with arrows, whereas arrowheads point to examples of double-labeled dendrites. Note that the majority of α subunit immunoreactive puncta are not associated with eGFP-positive dendrites; even in those cases when most somata are double-labeled (e.g., panels E or H). Scale bars: A-C 20 μm; D-O 10 μm.

Figure 3

Quantitative analysis of the distribution of α subunit variants in dorsal horn eGFP-positive neurons and in primary afferent terminals. **A-C**: Colocalization frequency of α subunit IR in vGluT2-eGFP **(A)**, GAD67-GFP **(B)** and GlyT2-eGFP **(C)** neurons, subdivided by lamina. The data are pooled from 2-3 mice per genotype. **D**: Percentage colocalization (mean ± SD) of CGRP- (lamina IIo), IB4- (lamina IIi), and CTB- (lamina III) positive primary afferent profiles with α subunit variants in C57BL/6J mice. **E**: Density of α subunit immunoreactive clusters (mean ± SD; n=3 mice/group) colocalized with CGRP-, IB4-, and CTB-positive profiles. Colocalization was quantified in six sections per mouse.

Figure 4

Immunohistochemical identification of α subunit-IR inside primary afferent terminals. **A:** Illustration of transganglionic and retrograde transport of CTB injected into the sciatic nerve. Note the extensive labeling of axons in the ipsilateral dorsal horn and neuronal somata in the ventral horn. **B:** Lamina-specific distribution of the three classes of primary afferents in the superficial dorsal horn, demonstrated by triple labeling for CGRP (peptidergic fibers; blue) in lamina IIo, IB4 (non-peptidergic fibers; green) in lamina Iii, and CTB-positive myelinated fiber terminals (magenta) in lamina III. **B'**: Triple labeling for CGRP (green), IB4 (blue) and PKCγ (magenta) confirmed the localization of non-peptidergic afferents in the outer part of lamina IIi. **C-F:** Representative images for double staining experiments depicting with high resolution the punctate distribution of α subunit IR (magenta) relative to afferent terminals (green), as well as their colocalization (white). Framed areas are enlarged in panels **G-J**. Scale, A, 200 μm; B: 20 μm; C-F: 5 μm; G-I: 0.5 μm.

Figure 5

Evidence for axo-axonic GABAergic synapses on primary afferent terminals. **A:** Postsynaptic distribution of gephyrin clusters (green) in the mouse spinal dorsal horn demonstrated by extensive apposition to presynaptic terminals positive for VIAAT (blue; arrow). **B:** Western blot analysis of gephyrin in crude mouse brain extracts and dorsal root ganglia. All bands, loaded with three different protein amounts, are from a single blot. C-G: Representative image showing the postsynaptic localization of α3 subunit and gephyrin clusters in primary afferent terminals apposed to a VIAAT-

positive terminal. Quadruple labeling was performed in fresh-frozen tissue to optimize detection of postsynaptic proteins. C: Quadruple staining for the α3 subunit (red), gephyrin (green), IB4 (blue) and VIAAT (orange); the stack of confocal images is displayed in the 3 Cartesian planes, with arrowheads pointing to axo-axonic synapses and the arrow to a terminal containing the α3 subunit, but not gephyrin, shown in 3D. **D:** Distribution of pixels depicting α3 subunit/gephyrin (yellow) and α3 subunit-IB4 (magenta) co-localization relative to primary afferents and VIAAT-positive terminals, showing quadruple labeling of axo-axonic synapses (white; arrowheads). **E-G**: Patterns of colocalization between pairs of markers depicted in color-separated panels, as indicated. Scale, A: 5 μm; C-G: 3 μm.

Table 1: Primary antibodies used

Target	Immunogen	Species	Source	Characterization	References
α1 subunit	Rat N-terminal synthetic peptide 1–16 (pGluPSQDELKDNTTVFTR)	Guinea pig serum	In house	Antibody and immunohistochemistry protocol were verified in mutant mice lacking the respective subunit	(Fritschy et al., 1997; Panzanelli et al., 2011; Schneider Gasser et al., 2007; Studer et al., 2006)
α2 subunit	Rat N-terminal synthetic peptide 1–9 (NIQEDEAKN)	Guinea pig affinity purified			
α3 subunit	Rat N-terminal synthetic peptide 1–15 (pGluGESRRQEPGDFVKQ)	Guinea pig serum			
α5 subunit	Rat N-terminal synthetic peptide 1–10 (QMPTSSVQDE)	Guinea pig serum			
α4 subunit	Rat N-terminal synthetic peptide 1–14 (LNESPGQNSKDEKL)	Rabbit affinity purified	Phosphosolutions, Aurora, CO; cat. no. 844-GA4N	Antibody and immunohistochemistry protocol were verified in $\alpha4^{-/-}$ mice	(Bencsits et al., 1999; Peng et al., 2002); Fritschy, unpublished
CGRP	Synthetic calcitonin gene related peptide	Rabbit polyclonal	Chemicon, Temecula, CA; cat no. AB15360	By immunohistochemistry both antibodies react with peptidergic primary afferent terminals. Specific reactivity of these antisera is eliminated by pre-incubation with excess peptide antigens	(Chang et al., 2004; Dirmeier et al., 2008)
Substance P	Substance P conjugated to BSA	Rat monoclonal	Bachem, St.Helen, UK; cat. no. T-1609		
Cholera toxin B	cholera toxin B subunit (cholerogenoid)	Goat serum	List Biological Laboratories, Campbell, CA; cat. no. 7032A6	immunoprecipitation of cholera toxin B subunit; selective detection of CTB injected into peripheral nerves; co-localization with vGluT2 in primary afferent terminals	(Todd et al., 2003)
Gephyrin	Affinity-purified rat glycine receptors	Mouse monoclonal, clone 7a	Synaptic Systems (Gottingen, Germany); cat. no. 147011	Selective detection of gephyrin in inhibitory synapses; detection of recombinant gephyrin expressed in neurons	(Pfeiffer et al., 1984; Sassoè-Pognetto et al., 2000)
GFP	Purified recombinant green fluorescent protein	Chicken IgY fraction from yolks	Aves laboratories, Portland, OR; cat. no. GFP-1020	Western blot analysis; immunohistochemistry using transgenic mice expression the GFP gene product.	(Encinas et al., 2006)
Protein kinase Cγ	Synthetic peptide 676-689 of human PKCγ (VNPDFVHPDARSPT)	Mouse monoclonal, clone 20	BD Transduction laboratories; cat no. 611158	Western blot analysis; immunohistochemistry	(Neumann et al., 2008)
Versican	recombinant protein fragment of GAG-α domain of mouse versican	Rabbit affinity purified	gift from Prof. Dieter Zimmermann	Immunoblotting of the fusion protein and crude mouse brain extracts; co-localization with IB4 in primary afferent terminals	(Schmalfeldt et al., 1998; Zimmermann et al., 1994)
VIAAT	Synthetic peptide 75-87 of rat VIAAT (AEPPVEGDIHYQR)	Rabbit affinity purified	Synaptic Systems; cat. no. 131003	Specific for the mammalian vGAT demonstrated by Western blotting and immunohistochemistry; selective detection of GABAergic terminals in	(Brünig et al., 2002; Fritschy et al., 2006; Panzanelli et al., 2009)

				brain sections and primary neuron cultures	
vGluT1	Recombinant GST-fusion protein containing amino acid residues 456-561 of rat vGluT1	Rabbit serum	Synaptic Systems; cat. no. 135002	Specific for the mammalian vGluT1 demonstrated by Western blotting and immunohistochemistry	(Bellocchio et al., 2000; Fujiyama et al., 2001; Todd et al., 2003)
vGluT2	Recombinant GST-fusion protein containing amino acid residues 510-582of rat vGluT2	Rabbit serum	Synaptic Systems; cat. no. 135102	Specific for the mammalian vGluT2 demonstrated by Western blotting and immunohistochemistry; selective detection of a subset of glutamatergic axon terminals in brain sections	(Fremeau et al., 2004; Nahmani and Erisir, 2005)

The non-peptidergic fibers were identified by the marker Isolectin B4-alexa 488 conjugate from Molecular probes, Eugene, OR, USA, cat no. 121411.

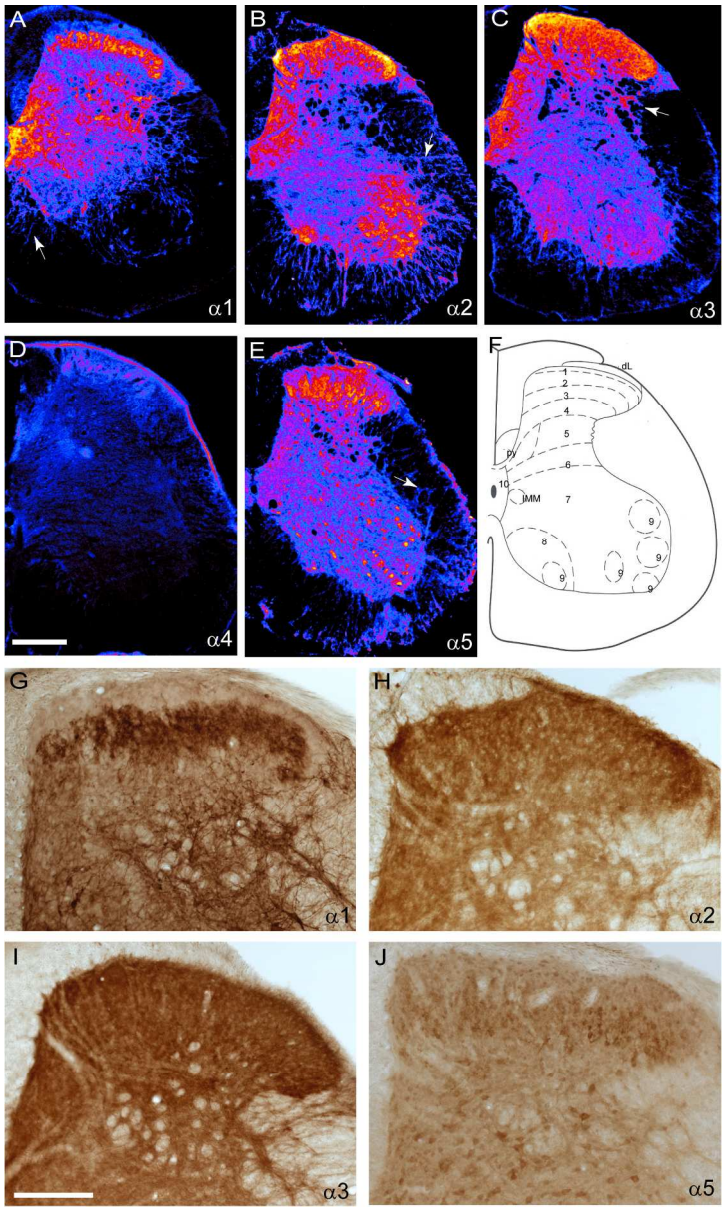

159x266mm (300 x 300 DPI)

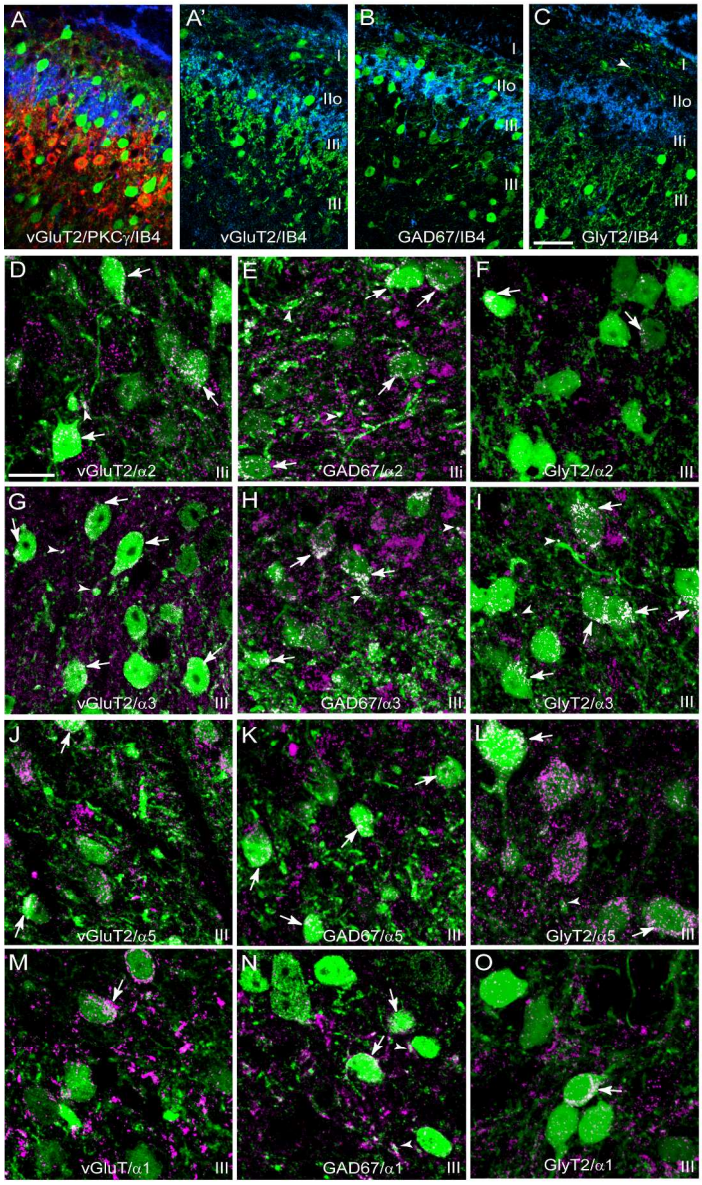

157x270mm (300 x 300 DPI)

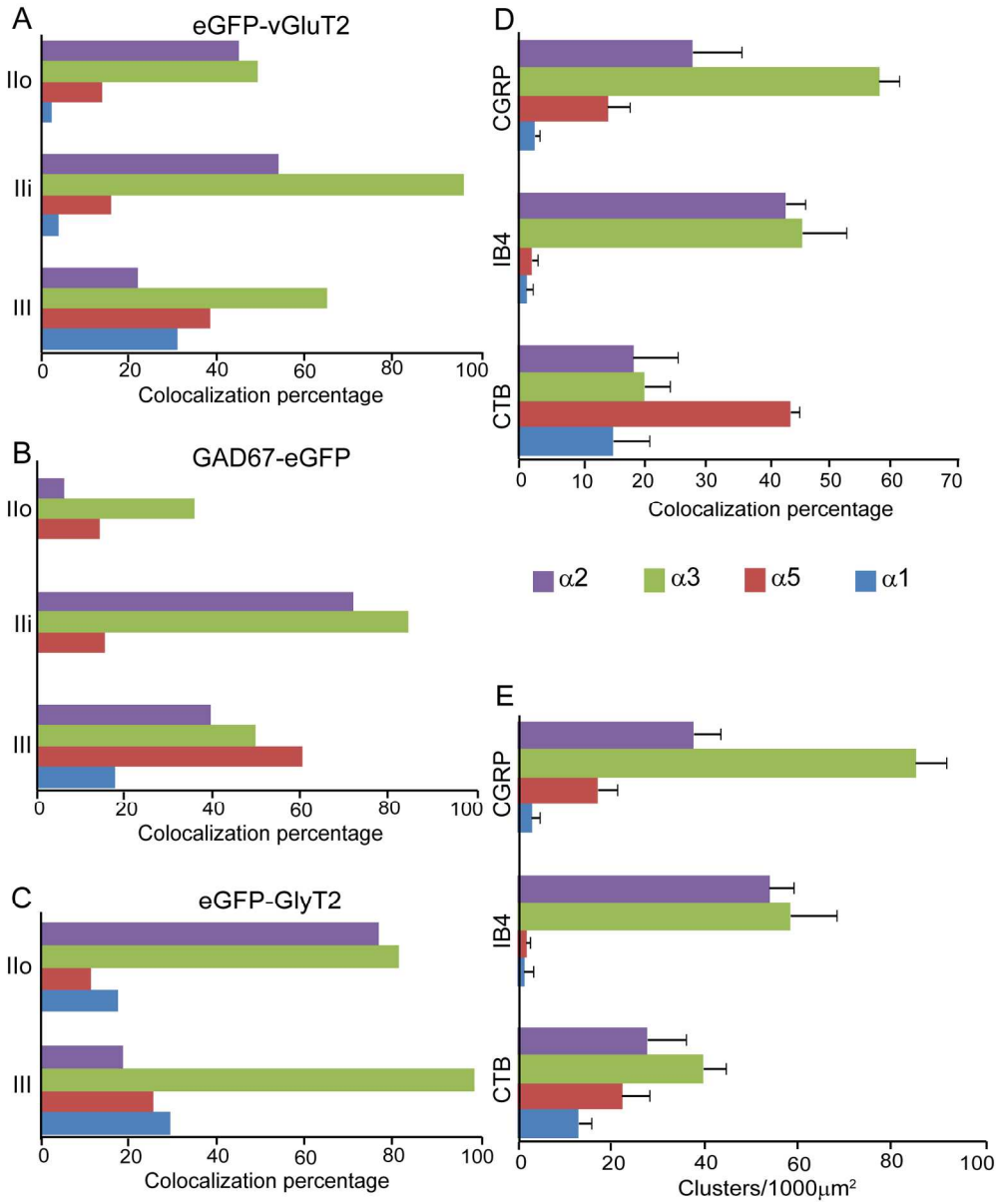

163x198mm (300 x 300 DPI)

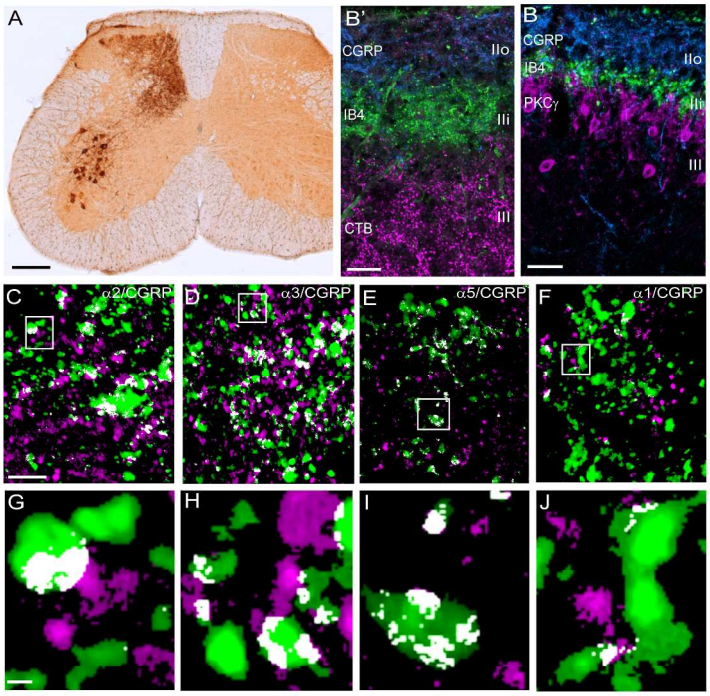

243x211mm (300 x 300 DPI)

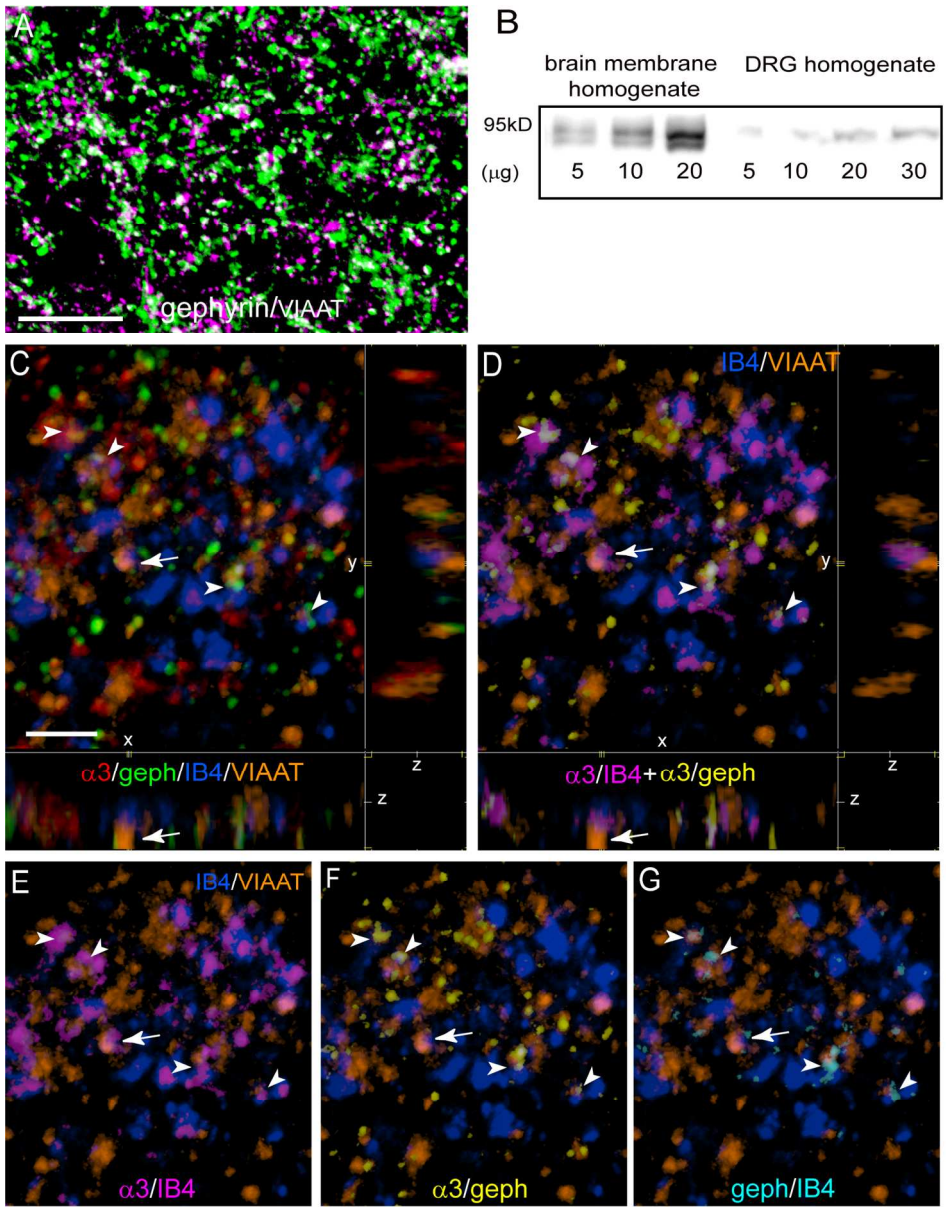

141x178mm (300 x 300 DPI)